BJR

https://doi.org/10.1259/bjr.20170767

Received: 10 October 2017 | Revised: 30 November 2017 | Accepted: 03 January 2018

Cite this article as:
Ando T, Kato H, Furui T, Morishige K-ichirou, Goshima S, Matsuo M. Uterine smooth muscle tumours with hyperintense area on T_1 weighted images: differentiation between leiomyosarcomas and leiomyomas. *Br J Radiol* 2018; **91**: 20170767.

FULL PAPER

Uterine smooth muscle tumours with hyperintense area on T_1 weighted images: differentiation between leiomyosarcomas and leiomyomas

[1]TOMOHIRO ANDO, MD, [1]HIROKI KATO, MD, [2]TATSURO FURUI, MD, [2]KEN-ICHIROU MORISHIGE, MD, [1]SATOSHI GOSHIMA, MD and [1]MASAYUKI MATSUO, MD

[1]Department of Radiology, Gifu University School of Medicine, Gifu, Japan
[2]Department of Obstetrics and Gynecology, Gifu University School of Medicine, Gifu, Japan

Address correspondence to: Dr Hiroki Kato
E-mail: *hkato@gifu-u.ac.jp*

Objective: Hyperintense area on T_1 weighted images (T_1 HIA) have been reported as suggestive features of uterine leiomyosarcoma (LMS), but differentiating LMS from leiomyoma (LM) is often difficult. This study aimed to evaluate the differences between uterine LMS and LM demonstrating intratumoral T_1 HIA.
Methods: MRI was performed in 509 patients with 1137 uterine smooth muscle tumours [14 LMSs, 5 smooth muscle tumours of uncertain malignant potential , and 1118 LMs] which exceeded 3 cm in diameter. LM with red degeneration and lipoleiomyoma were excluded from the study. We retrospectively reviewed the images and assessed T_1 HIA within tumours.
Results T_1 HIAs were observed in 11/14 (78.6%) LMSs, 0/5 (0%) smooth muscle tumours of uncertain malignant potential, and 15/1118 (1.3%) LMs. T_1 HIAs were more homogenous (53 *vs* 0%, $p < 0.01$) and more well-demarcated (60 *vs* 9%, $p < 0.05$) in LMs than in LMSs. T_2 hypointense rim within T_1 HIA (53 *vs* 9%, $p < 0.05$) was more frequently observed in LMs than in LMSs. The occupying rate of T_1 HIA (0.20 ± 0.24 *vs* 0.42 ± 0.27, $p < 0.05$) was smaller in LMs than in LMSs. The signal intensity ratio of T_1 HIA (1.83 ± 0.36 *vs* 1.38 ± 0.23, $p < 0.01$) was greater in LMs than in LMSs.
Conclusion: T_1 HIA within LM showed more homogeneity, better demarcation, smaller occupying rate, and higher signal intensity than T_1 HIA within LMS.
Advances in knowledge: The differences in T_1 HIA within tumours may be useful for differentiating between LMS and LM.

INTRODUCTION

Uterine leiomyosarcoma (LMS) is a rare aggressive mesenchymal tumour, and 5-year survival rates according to stages have been reported as follows: Stage I, 76%; Stage II, 60%; Stage III, 45%; and Stage IV, 29%.[1,2] In contrast, uterine leiomyoma (LM) is a common benign tumour that occurs in approximately 20–40% of reproductive-age females.[3] Pre-operative differential diagnosis between LMS and LM based solely on clinical features is very difficult.[1] MRI is a useful tool for tumour detection and characterization as well as for the assessment of disease staging.[1,4] However, it is also often difficult to distinguish LMS from LM using MR imaging because various degenerations, growth patterns, and complications occur in LM.[3–6]

Increased signal intensity on T_1 weighted images, moderate signal intensity on T_2 weighted images, and ill-demarcated margins have been reported as the most suggestive features of LMS.[4,6] Hyperintense area on T_1 weighted images (T_1 HIA) is also demonstrated in LM with red degeneration and lipoleiomyoma. Although T_1 HIA is the most important imaging finding of LMS, benign LM, excluding both LM with red degeneration and lipoleiomyomas, rarely demonstrates T_1 HIA. Therefore, if a uterine tumour demonstrates T_1 HIA within the tumour, radiologists often have difficulty differentiating between benign and malignant tumours. However, to our knowledge, no study has assessed detailed MR findings of uterine smooth muscle tumours with T_1 HIA. Thus, this study aimed to evaluate the differences in MR imaging findings between LMS and LM demonstrating T_1 HIA.

METHODS AND MATERIALS

Patients

The study was approved by the human research committee of our Institutional Review Board, and complied with the guidelines of the Health Insurance Portability and Accountability Act. The requirement for informed consent was

waived due to the retrospective nature of this study. We searched the electronic medical records at Gifu University Hospital for details of patients with histopathologically-proven uterine smooth muscle tumours, who pre-operatively underwent MRI between May 2005 and November 2016. After excluding patients with tumours <3 cm, 509 consecutive patients with uterine smooth muscle tumours [14 LMSs, 5 smooth muscle tumours of uncertain malignant potential (STUMPs), and 490 LMs] were included. Among these patients, 14 LMSs, 5 STUMPs, and 1118 LMs were recognized on MR images. Most patients underwent hysterectomy or myomectomy for tumour removal, but some LMs were incidentally found during hysterectomy performed for other diseases, such as endometrial cancer, cervical cancer, ovarian tumour, or advanced colorectal cancer.

MRI

MRI was performed using a 1.5 T MRI system (Intera Achieva 1.5 T Pulsar; Philips Medical Systems, Best, Netherlands) or a 3 T MRI system (Achieva Quasar Dual 3 T; Philips Medical Systems, Best, Netherlands). All MR images were obtained in the transverse plane at a section thickness of 5 mm with 2 mm intersection gap. Non-fat-suppressed T_1 weighted spin-echo images [repetition time/echo time (TR/TE, 556–782/10–17 ms; imaging matrices, 512 × 512; field of view, 26 × 26–32 × 32] cm, fat-suppressed T_1 weighted spin-echo images (TR/TE, 548–816/10–15 ms; imaging matrices, 512 × 512; field of view, 26 × 26–32 × 32 cm), and T_2 weighted fast spin-echo images (TR/TE, 4,412–7,402/90–100 ms; imaging matrices, 512 × 512; field of view, 26 × 26–32 × 32 cm) were obtained.

Image assessment

Two radiologists (with 18 and 4 years of post-training experience in genitourinary imaging), unaware of patient clinical and histopathological data, reviewed individually all MR images, and qualitative assessments were initially performed in a patient and were subsequently performed in another patient. Any disagreements of quantitative results between the two reviewers were resolved in consensus. When all qualitative assessments were finished, quantitative assessments were performed by the former (experienced reviewer) in a randomized fashion.

First, the reviewers assessed the presence of intratumoral T_1 HIA. T_1 HIA was visually defined as signal intensity higher than that in the skeletal muscles at the same level. T_1 HIA due to phase-encoded motion artefact or flow-related enhancement was carefully excluded. Second, if the reviewers confirmed the presence of T_1 HIA within the tumour, the presence of fat tissue on fat-suppressed T_1 weighted images was also evaluated. When T_1 HIA was caused by fat tissue, the tumour was defined as lipoleiomyoma. Subsequently, qualitative and quantitative assessments were performed for LMS with T_1 HIA and LM with T_1 HIA excluding LM with red degeneration and lipoleiomyoma.

As a qualitative assessment, the reviewers assessed the frequency, signal uniformity (homogeneous or heterogeneous), margin (well-demarcated or ill-demarcated), and distribution (central or peripheral) of intratumoral T_1 HIA. Central distribution was defined as centric location regardless of the square measure of intratumoral T_1 HIA, whereas peripheral distribution was defined as peripheral or eccentric location. The presence of T_2 hypointense rim within T_1 HIA, which was defined as ring-like hypointensity on T_2 weighted images along the periphery of T_1 HIA, was also evaluated.

As a quantitative assessment, the experienced reviewer measured the maximum diameters of the tumours and counted the number of T_1 HIAs. The square measure of both T_1 HIA and whole tumour were also measured using commercially available Digital Imaging and Communications in Medicine viewers, and the occupying rates were calculated as the T_1 HIA-to-whole tumour square measure ratio. In addition, the reviewer defined regions of interest (ROIs) within T_1 HIA and recorded the signal intensities. ROIs were placed to encompass T_1 HIA and conform to the shape of T_1 HIA as much as possible (Figure 1a). Signal intensities of the skeletal muscle (iliopsoas muscle or gluteal muscle) with as little intramuscular fat as possible at the same level of T_1 HIA were also measured (Figure 1a). The reviewer copied the ROIs of both T_1 HIA and the skeletal muscle, pasted them on the same level of T_2 weighted images (Figure 1b), and calculated them as the T_1 HIA-to-skeletal muscle signal intensity ratio on T_1 and T_2 weighted images.

Statistical analysis

All statistical analyses were performed using SPSS v. 22.0 (SPSS, Inc, an IBM Company, Chicago, IL). The χ^2 test or Fisher exact test was performed to compare the qualitative results (frequency, signal uniformity, margin, distribution of T_1 HIA, and T_2 hypointense rim within T_1 HIA) between LMS with T_1 HIA and LM with T_1 HIA excluding LM with red degeneration and lipoleiomyoma. The unpaired *t*-test was used to compare the quantitative results (age, maximum diameter of tumour, number of T_1 HIAs, occupying rate of T_1 HIA, and signal intensity ratio of T_1 HIA on T_1 and T_2 weighted images) between LMS with T_1 HIA and LM with T_1 HIA excluding LM with red degeneration and lipoleiomyoma. Variables with *p*-values <0.05 in each quantitative analysis of MR findings were chosen for multiple logistic regression analysis.

RESULTS

Intratumoral T_1 HIA was revealed in 30 benign smooth muscle tumours of the uterus. Among them, 11 LMs with red degeneration and 4 with lipoleiomyomas, as confirmed by pathological examination or typical MR findings, were excluded from the study. In total, T_1 HIAs were observed in 11/14 (78.6%) LMSs, 0/5 (0%) STUMPs, and 15/1118 (1.3%) LMs (Table 1). Thus, qualitative and quantitative assessments were performed for 11 LMSs with T_1 HIA and 15 LMs with T_1 HIA excluding LMs with red degeneration and lipoleiomyomas. Patient characteristics accompanied by T_1 HIA are summarized in Table 2.

Qualitative imaging findings and quantitative measurements of LMSs and LMs demonstrating T_1 HIA are summarized in Table 3. T_1 HIAs were more homogeneous (53 *vs* 0%, $p < 0.01$) and more well-demarcated (60 *vs* 9%, $p < 0.05$) in LMs than in LMSs (Figures 1–5). T_2 hypointense rims within T_1 HIA (53 *vs* 9%, $p < 0.05$) were more frequently observed in LMs than in

Figure 1. A 48-year-old female with uterine leiomyoma. (a) T_1 weighted spin-echo image (TR/TE, 728/10 ms) shows a homogeneous, well-demarcated, peripheral, moderately hyperintense area (arrow). The experienced reviewer placed ROIs to encompass T_1 HIA and conform to the shape of T_1 HIA as much as possible (black dotted circle) and on the skeletal muscle as little intramuscular fat as possible at the same level of T_1 HIA (white dotted circle). (b) T_2 weighted fast spin-echo image (TR/TE, 4500/108 ms) shows a heterogeneously hyperintense lesion (arrow) within the myometrium of uterine body. The reviewer copied these ROIs of both T_1 HIA and the skeletal muscle and pasted on the same level of T_2 weighted images (dotted circles). T_1 HIA, hyperintense area on T_1 weighted images; ROIs, regions of interest; TE, echo time; TR, repetition time.

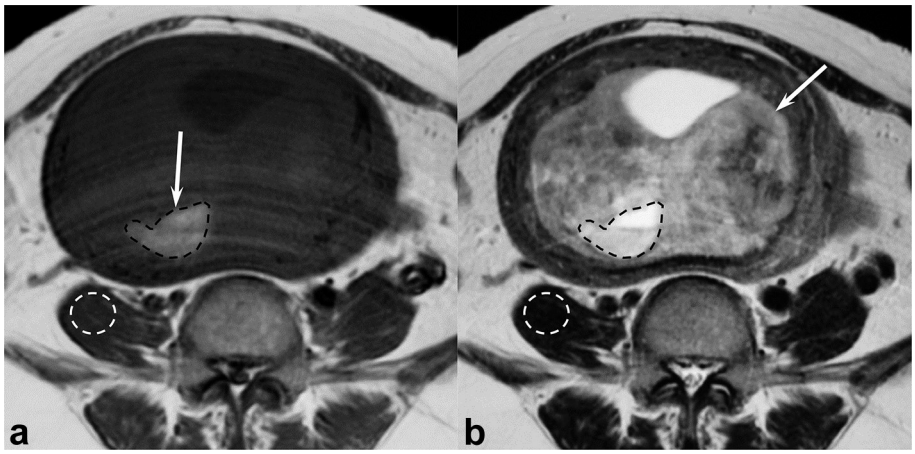

LMSs (Figures 1–5). No significant difference was observed in central distribution (53 *vs* 18%, $p = 0.078$) between LMs and LMSs.

Patients with LMs were younger than those with LMSs (42.4 ± 5.7 *vs* 59.5 ± 11.4 years, $p < 0.01$), and maximum tumor diameter was smaller (87.9 ± 31.9 *vs* 114.7 ± 33.533.6 mm, $p < 0.05$) in LMs than in LMSs. The occupying rate of T_1 HIA (0.20 ± 0.24 *vs* 0.42 ± 0.27, $p < 0.05$) were smaller in LMs than in LMSs (Figures 1–5). The signal intensity ratio of T_1 HIA (1.83 ± 0.36 *vs* 1.38 ± 0.23, $p < 0.01$) was greater in LMs than in LMSs (Figures 1–5). No significant difference was observed in the number of T_1 HIAs (2.00 ± 1.77 *vs* 2.36 ± 1.80, $p = 0.613$) or in the signal intensity ratio of T_1 HIA on T_2 weighted images (5.90 ± 3.79 *vs* 5.61 ± 2.24, $p = 0.826$).

The multiple logistic regression analysis showed that the higher signal intensity ratio of T_1 HIA on T_1 weighted images was significantly correlated with the presence of LM (odds ratio, 312.0; $p < 0.05$).

Table 1. The frequencies of T_1 HIA in uterine smooth muscle tumours

	LMS	STUMP	LM
Number of patients	14	5	490
Number of tumours	14	5	1118
Tumours with T_1 HIA	11	0	15
Frequency	78.6%	0%	1.3%

HIA, hyperintense area; LM, leiomyoma; LMS, leiomyosarcoma; STUMP, smooth muscle tumour of uncertain malignant potential; T_1 HIA, HIA on T_1 weighted images.
These tumours exceeded 3 cm in diameter. LM with red degeneration ($n = 11$) and lipoleiomyoma ($n = 4$) accompanied by T_1 HIA were excluded.

DISCUSSION

One of the characteristic MR findings of LMS is T_1 HIA.[4,6–8] However, LM with red degeneration and lipoleiomyoma also demonstrates intratumoral T_1 HIA. Red degeneration is a haemorrhagic infarction known to result from venous occlusion and is associated with pregnancy, oral contraceptive use, gonadotropin-releasing hormone agonist therapy, and/or torsion of pedunculated leiomyomas.[3,5,9,10] Unlike other types of degeneration, red degeneration usually causes systemic symptoms, such as low abdominal pain, pyrexia, and leukocytosis[5,11] and typically exhibits peripheral rim-like or diffuse T_1 HIA and variable signal intensity with or without T_2 hypointense rim.[3,5,10,12,13] Therefore,

Table 2. Patient characteristics accompanied by T_1 HIA

Characteristics	LMS with T_1 HIA	LM with T_1 HIA
Number of patients/tumour	11	15
Age (year)		
Range	43–74	27–4
Mean	59.5	42.4
Menstruation		
Pre-menopausal	3	14
Post-menopausal	8	1
Hormonal therapy		
None	11	10
Oral contraceptives	0	2
GnRH agonist	0	3

HIA, hyperintense area; LM, leiomyoma; LMS, leiomyosarcoma; GnRH, gonadotropin-releasing hormone; T_1 HIA, HIA on T_1 weighted images.

Table 3. Qualitative imaging findings and quantitative measurements of LMSs and LMs accompanied by T_1 HIA

	LMS with T_1 HIA (n = 11)	LM with T_1 HIA (n = 15)	p-value
Qualitative imaging findings of T_1 HIA			
Homogeneous	0 (0)	8 (53)	0.004[a]
Well-demarcated	1 (9)	9 (60)	0.011[a]
Central distribution	2 (18)	8 (53)	0.078
T_2 hypointense rim	1 (9)	8 (53)	0.024[a]
Quantitative measurements			
Age of patients	59.5 ± 11.4 (43–74)	42.4 ± 5.7 (27–54)	<0.001[a]
Maximum diameter of tumour	114.7 ± 33.6 (62–179)	87.9 ± 31.9 (40–146)	0.049[a]
Number of T_1 HIA	2.36 ± 1.80 (1–7)	2.00 ± 1.77 (1–7)	0.613
Occupying rate of T_1 HIA	0.42 ± 0.27 (0.08–0.98)	0.20 ± 0.24 (0.01–0.69)	0.038[a]
Signal intensity ratio of T_1 HIA			
T_1 weighted images	1.38 ± 0.23 (1.18–1.91)	1.83 ± 0.36 (1.25–2.59)	<0.001[a]
T_2 weighted images	5.61 ± 2.24 (3.06–8.66)	5.90 ± 3.79 (1.11–16.81)	0.826

HIA, hyperintense area; LM, leiomyoma; LMS, leiomyosarcoma; T_1 HIA, HIA on T_1 weighted images.
In qualitative imaging findings, data are numbers of patients, and numbers in parentheses are frequencies expressed as percentages. In quantitative measurements, data are age, maximum diameter of tumour, number of T_1 HIA, occupying rate of T_1 HIA, and signal intensity ratio of T_1 HIA on T_1 and T_2 weighted images, with the mean ± 1 standard deviation, and numbers in parentheses are range of numbers.
[a]Significant difference in frequency or value was found between LMS and LM.

radiologists can easily diagnose red degeneration using both clinical presentation and characteristic MR findings. Meanwhile, T_1 HIA in lipoleiomyoma corresponds with fatty components and fat-saturated sequences are helpful in diagnosing lipoleiomyoma.[14,15] If LM with red degeneration and lipoleiomyoma demonstrates characteristic MR findings, malignancy can be ruled out. Thus, we excluded LM with red degeneration and lipoleiomyoma in the present study. However, even though LM with red degeneration and lipoleiomyoma are excluded, benign uterine LMs rarely demonstrate T_1 HIA within the tumours.

Histopathologically, tumour necrosis is frequently observed within both LMS and LM, but considerable differences exist between the two pathologies. Although several types of necrosis are found in uterine smooth muscle tumours, they are roughly divided into two types: coagulative necrosis (tumour cell necrosis) and infarct-type necrosis (hyaline necrosis). Coagulative necrosis, which is common in LMS, is characterized by an abrupt transition from viable to non-viable areas, without interposed inflammation, granulation, or hyalinized tissue.[16,17] On the other hand, infarct-type necrosis, which is common in LM, is characterized by the presence of either granulation tissue or hyalinization between viable and non-viable areas and is frequently associated with recent or old haemorrhage.[16,17] Coagulative necrosis is observed only in LMS;[16–18] therefore, it is considered an important pathological finding for diagnosing

Figure 2. A 43-year-old female with uterine leiomyoma. (a) T_1 weighted spin-echo image (TR/TE, 728/12 ms) shows a homogeneous, well-demarcated, peripheral, moderately hyperintense area (arrow) within the tumour (signal intensity ratio of T_1 HIA: 1.74). (b) Fat-suppressed T_1 weighted spin-echo image (TR/TE, 758/12 ms) clearly demonstrates intratumoral hyperintense area (arrow) compared with non-fat-suppressed T_1 weighted image. (c) T_2 weighted fast spin-echo image (TR/TE, 4412/100 ms) shows a heterogeneously hypointense lesion (arrow) within the myometrium of uterine body. Peripherally located focal area with hypointense rim is observed at the same site of T_1 HIA (arrow head). T_1 HIA = HIA on T_1 weighted images; TE, echo time; TR, repetition time.

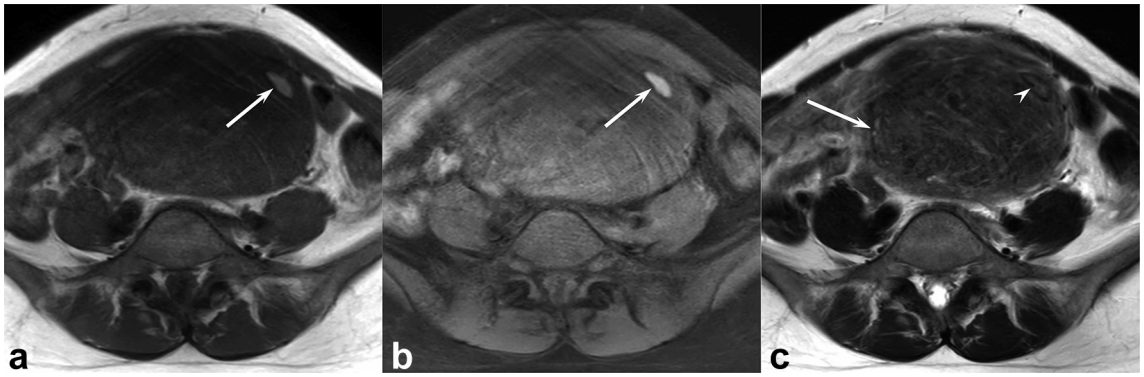

Figure 3.A 27-year-old female with uterine leiomyoma. (a) T_1 weighted spin-echo image (TR/TE, 728/10 ms) shows heterogeneous, ill-demarcated, central, moderately hyperintense areas (arrows) within the tumour (signal intensity ratio of T_1 HIA: 1.94). (b) T_2 weighted fast spin-echo image (TR/TE, 5298/100 ms) shows a heterogeneously hyperintense lesion (arrow) within the myometrium of uterine body. Centrally located focal areas with hypointense rim are observed at the same site of T_1 HIA (arrow heads). T_1 HIA = HIA on T_1 weighted images; TE, echo time; TR, repetition time.

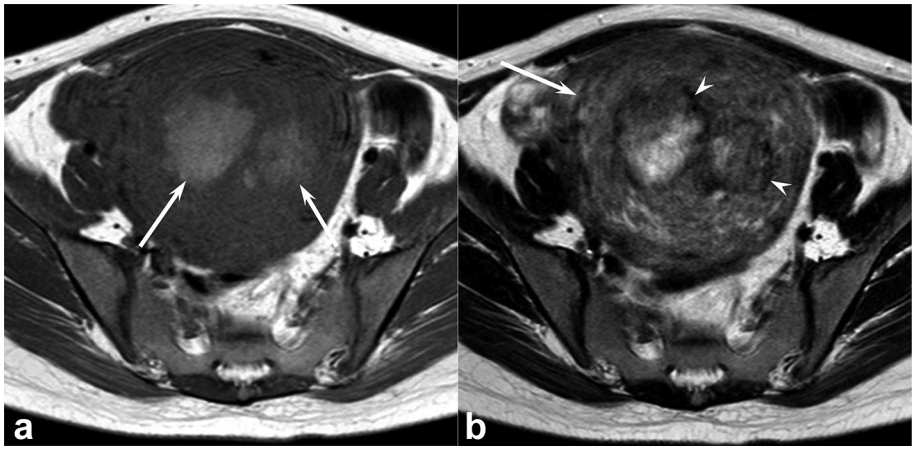

LMS.[16–21] Although the distinction between coagulative necrosis and infarct-type necrosis is usually straightforward, the difficulty in the reliable histopathological distinction between the two has been reported.[16,17,19,21]

T_1 HIA within LMS corresponds with intratumoral coagulative necrotic foci,[6,9] whereas that within LM corresponds with hyaline necrosis with associated recent or old haemorrhage. In our series, the MR characteristics of T_1 HIA were considerably different in signal uniformity, margin, T_2 hypointense rim, occupying rate, and signal intensity ratio between LMS and LM. Specifically, T_1 HIA within LMS showed more heterogeneity, more ill-demarcation, larger occupying rate, and lower signal intensity than T_1 HIA within LM. The larger occupying rate of T_1 HIA within LMS suggested widespread distribution of coagulative necrosis. The signal intensity ratio of T_1 HIA was greater in LMs than in LMSs, because the concentration of blood products (haemoglobin) tended to occur in LMs. T_2 hypointense rim within T_1 HIA, which was more frequently observed in LM, corresponded with hemosiderin deposition and suggested long-standing intratumoral haemorrhage.

The present study has several limitations. First, the study population was small as the study was conducted at a single institution (Gifu University Hospital). Especially, because LMS is a potentially rare tumour, the numbers of LMS are too small in the present study. Second, two different MRI scanners were used because of the retrospective nature of this study. However, we believe that the results would not have differed considerably if we obtained images using the same MRI scanner, because only conventional MR sequences were assessed in this study. Third, we assessed only conventional unenhanced MR images and did not evaluate contrast-enhanced images and diffusion-weighted images. However, we believe that these simple results will contribute to clinical practice in the

Figure 4. A 47-year-old female with uterine leiomyosarcoma. (a) T_1 weighted spin-echo image (TR/TE, 668/10 ms) shows a heterogeneous, ill-demarcated, peripheral, slightly hyperintense area (arrow) within the tumour (signal intensity ratio of T_1 HIA: 1.26). (b) Fat-suppressed T_1 weighted spin-echo image (TR/TE, 748/10 ms) clearly demonstrates intratumoral hyperintense area (arrow) compared with non-fat-suppressed T_1 weighted image. (c) T_2 weighted fast spin-echo image (TR/TE, 4856/100 ms) shows a well-demarcated, heterogeneously hyperintense lesion (arrow) within the myometrium of uterine body. A focal area with hypointense rim is not observed. T_1 HIA = HIA on T_1 weighted images; TE, echo time; TR, repetition time.

Figure 5. A 63-year-old female with uterine leiomyosarcoma. (a) T_1 weighted spin-echo image (TR/TE, 816/8 ms) shows heterogeneous, ill-demarcated, peripheral, slightly hyperintense areas (arrows) within the tumour (signal intensity ratio of T_1 HIA: 1.32). (b) T_2 weighted fast spin-echo image (TR/TE, 3883/119 ms) shows a well-demarcated, heterogeneously hyperintense lesion (arrow) within the myometrium of uterine body. A focal area with hypointense rim is not observed. T_1 HIA = HIA on T_1 weighted images; TE, echo time; TR, repetition time.

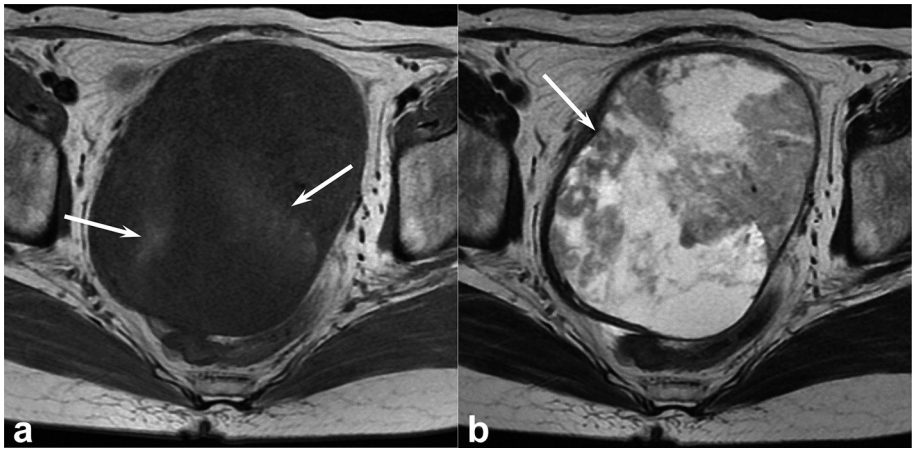

radiological differentiation of LMS from LM. Fourth, because STUMP demonstrating T_1 HIA was not observed in this study, further investigation is warranted to determine the characteristic imaging findings of STUMP.

CONCLUSIONS

In this study, T_1 HIA within LM showed more homogeneity, better demarcation, smaller occupying rate, and higher signal intensity than T_1 HIA within LMS. T_2 hypointense rim within T_1 HIA was more frequently found in LM than in LMS. These differences of MRI findings may be useful for differential diagnosis between LMS and LM in addition to the difference of patients' ages and menstrual status. Therefore, if a uterine tumour demonstrates T_1 HIA within the tumour radiologists should keep in mind the differences of MRI findings between LMS and LM.

REFERENCES

1. Santos P, Cunha TM. Uterine sarcomas: clinical presentation and MRI features. *Diagn Interv Radiol* 2015; **21**: 4–9. doi: https://doi.org/10.5152/dir.2014.14053
2. Ricci S, Stone RL, Fader AN. Uterine leiomyosarcoma: epidemiology, contemporary treatment strategies and the impact of uterine morcellation. *Gynecol Oncol* 2017; **145**: 208–16. doi: https://doi.org/10.1016/j.ygyno.2017.02.019
3. Bolan C, Caserta MP. MR imaging of atypical fibroids. *Abdom Radiol* 2016; **41**: 2332–49. doi: https://doi.org/10.1007/s00261-016-0935-0
4. Arleo EK, Schwartz PE, Hui P, McCarthy S. Review of leiomyoma variants. *AJR Am J Roentgenol* 2015; **205**: 912–21. doi: https://doi.org/10.2214/AJR.14.13946
5. Ueda H, Togashi K, Konishi I, Kataoka ML, Koyama T, Fujiwara T, et al. Unusual appearances of uterine leiomyomas: MR imaging findings and their histopathologic backgrounds. *Radiographics* 1999; **19**: S131–S145. doi: https://doi.org/10.1148/radiographics.19.suppl_1.g99oc04s131
6. Goto A, Takeuchi S, Sugimura K, Maruo T. Usefulness of Gd-DTPA contrast-enhanced dynamic MRI and serum determination of LDH and its isozymes in the differential diagnosis of leiomyosarcoma from degenerated leiomyoma of the uterus. *Int J Gynecol Cancer* 2002; **12**: 354–61. doi: https://doi.org/10.1046/j.1525-1438.2002.01086.x
7. Sahdev A, Sohaib SA, Jacobs I, Shepherd JH, Oram DH, Reznek RH. MR imaging of uterine sarcomas. *AJR Am J Roentgenol* 2001; **177**: 1307–11. doi: https://doi.org/10.2214/ajr.177.6.1771307
8. Tirumani SH, Ojili V, Shanbhogue AK, Fasih N, Ryan JG, Reinhold C. Current concepts in the imaging of uterine sarcoma. *Abdom Imaging* 2013; **38**: 397–411. doi: https://doi.org/10.1007/s00261-012-9919-x
9. Tanaka YO, Nishida M, Tsunoda H, Okamoto Y, Yoshikawa H. Smooth muscle tumors of uncertain malignant potential and leiomyosarcomas of the uterus: MR findings. *J Magn Reson Imaging* 2004; **20**: 998–1007. doi: https://doi.org/10.1002/jmri.20207
10. Hachiya K, Kato H, Kawaguchi S, Kojima T, Nishikawa Y, Fujiwara S, et al. Red degeneration of a uterine fibroid following the administration of gonadotropin releasing hormone agonists. *J Obstet Gynaecol* 2016; **36**: 1018–9. doi: https://doi.org/10.1080/01443615.2016.1234449
11. Phelan JP. Myomas and pregnancy. *Obstet Gynecol Clin North Am* 1995; **22**: 801–5.
12. Kawakami S, Togashi K, Konishi I, Kimura I, Fukuoka M, Mori T, et al. Red degeneration of uterine leiomyoma: MR appearance. *J Comput Assist Tomogr* 1994; **18**: 925–8.
13. Murase E, Siegelman ES, Outwater EK, Perez-Jaffe LA, Tureck RW. Uterine leiomyomas: histopathologic features, MR imaging findings, differential diagnosis, and treatment. *Radiographics* 1999; **19**: 1179–97. doi: https://doi.org/10.1148/radiographics.19.5.g99se131179
14. Aizenstein R, Wilbur AC, Aizenstein S. CT and MRI of uterine lipoleiomyoma. *Gynecol Oncol* 1991; **40**: 274–6. doi: https://doi.org/10.1016/0090-8258(90)90291-R

15. Tsushima Y, Kita T, Yamamoto K. Uterine lipoleiomyoma: MRI, CT and ultrasonographic findings. *Br J Radiol* 1997; **70**: 1068–70. doi: https://doi.org/10.1259/bjr.70.838.9404215
16. Toledo G, Oliva E. Smooth muscle tumors of the uterus: a practical approach. *Arch Pathol Lab Med* 2008; **132**: 595–605. doi: https://doi.org/10.1043/1543-2165(2008)132[595:SMTOTU]2.0.CO;2
17. Oliva E. Practical issues in uterine pathology from banal to bewildering: the remarkable spectrum of smooth muscle neoplasia. *Mod Pathol* 2016; **29**(Suppl 1): S104–S120. doi: https://doi.org/10.1038/modpathol.2015.139
18. Kempson RL, Hendrickson MR. Smooth muscle, endometrial stromal, and mixed Müllerian tumors of the uterus. *Mod Pathol* 2000; **13**: 328–42. doi: https://doi.org/10.1038/modpathol.3880055
19. Bell SW, Kempson RL, Hendrickson MR. Problematic uterine smooth muscle neoplasms. A clinicopathologic study of 213 cases. *Am J Surg Pathol* 1994; **18**: 535–58.
20. Amant F, Moerman P, Vergote I. Report of an unusual problematic uterine smooth muscle neoplasm, emphasizing the prognostic importance of coagulative tumor cell necrosis. *Int J Gynecol Cancer* 2005; **15**: 1210–2. doi: https://doi.org/10.1111/j.1525-1438.2005.00183.x
21. Lim D, Alvarez T, Nucci MR, Gilks B, Longacre T, Soslow RA, et al. Interobserver variability in the interpretation of tumor cell necrosis in uterine leiomyosarcoma. *Am J Surg Pathol* 2013; **37**: 650–8. doi: https://doi.org/10.1097/PAS.0b013e3182851162